YbeA is the $m^3\Psi$ methyltransferase RlmH that targets nucleotide 1915 in 23S rRNA

ELZBIETA PURTA,[1,2] KATARZYNA H. KAMINSKA,[2,3] JOANNA M. KASPRZAK,[3] JANUSZ M. BUJNICKI,[2,3] and STEPHEN DOUTHWAITE[1]

[1]Department of Biochemistry and Molecular Biology, University of Southern Denmark, DK-5230 Odense M, Denmark
[2]Laboratory of Bioinformatics and Protein Engineering, International Institute of Molecular and Cell Biology in Warsaw, 02-109 Warsaw, Poland
[3]Laboratory of Bioinformatics, Institute of Molecular Biology and Biotechnology, Faculty of Biology, Adam Mickiewicz University, 61-614 Poznan, Poland

ABSTRACT

Pseudouridines in the stable RNAs of Bacteria are seldom subjected to further modification. There are 11 pseudouridine (Ψ) sites in *Escherichia coli* rRNA, and further modification is found only at Ψ1915 in 23S rRNA, where the N-3 position of the base becomes methylated. Here, we report the identity of the *E. coli* methyltransferase that specifically catalyzes methyl group addition to form $m^3\Psi$1915. Analyses of *E. coli* rRNAs using MALDI mass spectrometry showed that inactivation of the *ybeA* gene leads to loss of methylation at nucleotide Ψ1915. Methylation is restored by complementing the knockout strain with a plasmid-encoded copy of *ybeA*. Homologs of the *ybeA* gene, and thus presumably the ensuing methylation at nucleotide $m^3\Psi$1915, are present in most bacterial lineages but are essentially absent in the Archaea and Eukaryota. Loss of *ybeA* function in *E. coli* causes a slight slowing of the growth rate. Phylogenetically, *ybeA* and its homologs are grouped with other putative S-adenosylmethionine-dependent, SPOUT methyltransferase genes in the Cluster of Orthologous Genes COG1576; *ybeA* is the first member to be functionally characterized. The YbeA methyltransferase is active as a homodimer and docks comfortably into the ribosomal A site without encroaching into the P site. YbeA makes extensive interface contacts with both the 30S and 50S subunits to align its active site cofactor adjacent to nucleotide Ψ1915. Methylation by YbeA (redesignated RlmH for *r*RNA *l*arge subunit *m*ethyltransferase *H*) possibly functions as a stamp of approval signifying that the 50S subunit has engaged in translational initiation.

Keywords: RNA mass spectrometry; helix 69; pseudouridine methylation; RluD; ribosomal subunit interface

INTRODUCTION

The pivotal roles carried out by rRNAs during protein synthesis on the ribosome (Noller 2005) are supported by a range of nucleotide modifications that are added post-transcriptionally (Grosjean 2005). In *Escherichia coli* there are 11 modified nucleotides in 16S rRNA and 25 in 23S rRNA, and these modifications consist almost exclusively of pseudouridines and methylations on bases and ribose (Rozenski et al. 1999; Ofengand and Del Campo 2004; Andersen and Douthwaite 2006). In principle, methylation and pseudouridylation have opposing effects on the structure of the rRNA and its interactions with other ribosomal components. Base methylation creates a hydrophobic patch that improves the potential for base stacking, but removes an electrostatic interaction site and might sterically hinder the close approach of other components or ligands; ribose methylation can have similar effects while at the same time stabilizing the phosphodiester backbone. Pseudouridines, on the other hand, gain an extra site for electrostatic interaction after the N1-nitrogen, which was originally an integral part of the uridine glycosidic bond, swaps its role with the C5-carbon and becomes free to make a hydrogen bond. Notably, the N3-nitrogen remains in the same position in both uridine and pseudouridine (Fig. 1). Methylation and pseudouridylation rarely happen together at the same nucleotide, and in *Escherichia coli* RNAs there

Reprint requests to: Stephen Douthwaite, Department of Biochemistry and Molecular Biology, University of Southern Denmark, Campusvej 55, DK-5230 Odense M, Denmark; e-mail: srd@bmb.sdu.dk; fax: +45 6550 2467.

Abbreviations: AdoMet, S-adenosylmethionine; COG, Cluster of Orthologous Genes; MALDI, matrix assisted laser desorption/ionization; MS, mass spectrometry; m^3U, 3-methyluridine; $m^3\Psi$, 3-methylpseudouridine; *m/z*, mass (in daltons) to charge ratio; RFM, Rossmann-fold methyltransferase; *rlmH*, rRNA large subunit methyltransferase gene *H* (synonym, *ybeA*); SPOUT, SpoU and TrmD methyltransferases.

Article published online ahead of print. Article and publication date are at http://www.rnajournal.org/cgi/doi/10.1261/rna.1198108.

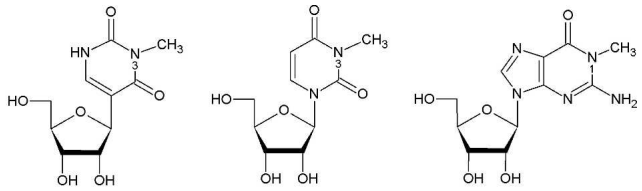

FIGURE 1. Chemical structures of 3-methylpseudoridine (m$^3\Psi$), 3-methyluridine (m^{3}U), and 1-methylguanosine (m^{1}G).

is but a single example: of the 11 pseudouridines in *E. coli* rRNA, only position 1915 is subjected to further modification, and this occurs via addition of a methyl group to the base N-3 position to form m$^3\Psi$1915 (Kowalak et al. 1996).

The mechanisms by which rRNAs are post-transcriptionally modified in Bacteria are fundamentally different from those operating in Archaea and Eukaryota. Pseudouridylations and 2′-*O*-methylations make up the bulk of eukaryal rRNA modifications, and most are added by modification enzymes that are not specific by themselves but need to be guided to target nucleotides by complementary sequences in snoRNAs (Lafontaine and Tollervey 1998; Kiss 2001). Comparable mechanisms have more recently been found in the Archaea (Tran et al. 2004). In contrast, Bacteria lack such guide RNAs and, consequently, each bacterial rRNA methylation requires its own specific enzyme (Andersen and Douthwaite 2006; Sergiev et al. 2007). The requirements for synthesis of pseudouridines in Bacteria are (almost) as stringent. For instance, *E. coli* pseudouridine synthases are usually specific for one uridine or a limited set of uridines that occupy a similar structural context (Ofengand and Del Campo 2004); and this latter type is exemplified by RluD, which converts 23S rRNA nucleotides U1911, U1915 and U1917 to pseudouridines.

Modifications in rRNA generally cluster within regions of the ribosome that perform key functions (Brimacombe et al. 1993; Decatur and Fournier 2002; Ofengand and Del Campo 2004) and Ψ1911, Ψ1915, and Ψ1917 are no exception. These nucleotides are located at the end of hairpin 69, where they are exposed to the solvent at the 50S subunit interface (Ban et al. 2000; Harms et al. 2001); hairpin 69 interacts with helix 44 in 16S rRNA to form interbridge B2a during association with the 30S subunit (Yusupov et al. 2001; Schuwirth et al. 2005; Korostelev et al. 2006; Selmer et al. 2006). Various studies have demonstrated the functional importance of hairpin 69 (Ali et al. 2006) and of individual nucleotides within this hairpin (O'Connor and Dahlberg 1995; Liiv et al. 2005; Hirabayashi et al. 2006; O'Connor 2007) and the modifications at these nucleotides (Gutgsell et al. 2001; Johansen et al. 2006; Ejby et al. 2007). However, the exact role of m$^3\Psi$1915 remains to be established, as does the identity of the methyltransferase that modifies this nucleotide.

It was speculated recently that the putative methyltransferase YbeA might be responsible for the m$^3\Psi$1915 methylation (Tkaczuk et al. 2007). Bioinformatics analyses showed that YbeA belongs to the Cluster of Orthologous Genes COG1576, within the SPOUT superfamily of AdoMet-dependent RNA methyltransferases (Tkaczuk et al. 2007). No member of COG1576 had yet been functionally characterized, although their closest relatives in the SPOUT superfamily are the TrmD-type m^{1}G methyltransferases (COG0336) and, slightly more distant, the Trm10p-type m^{1}G methyltransferases (COG2419). The SPOUT superfamily also includes RlmE-type m^{3}U methyltransferases (COG1385). The m^{3}U and m^{1}G methyltransferases modify equivalent nitrogen atoms in uracil and the pyrimidine ring of guanine (Fig. 1). As none of the m^{1}G RNA methyltransferases remain undiscovered in *E. coli*, YbeA was viewed as a reasonable candidate for the m$^3\Psi$1915 methylation.

In this study, we used MALDI mass spectrometry to compare the rRNA methylation pattern in a *ybeA*-knockout strain to that in wild-type *E. coli* cells. A recombinant version of the enzyme was expressed in the knockout strain to determine whether the original wild-type rRNA methylation pattern could be restored. These experiments show unequivocally that YbeA catalyzes the m$^3\Psi$1915 methylation. Docking simulations indicate that YbeA binds as a homodimer to the ribosomal A site at the interface between the 30S and 50S subunits and recognizes its substrate in a manner that has not previously been seen among the rRNA methyltransferases.

RESULTS AND DISCUSSION

In silico identification of YbeA as an m$^3\Psi$ RNA methyltransferase candidate

Methylation at the N3 of pseudouridine has been observed only at nucleotide m$^3\Psi$1915 in 23S rRNA, and at present this modification appears to be unique. Thus, with no enzyme precedent for m$^3\Psi$ methylation, we looked at enzyme groups that are phylogenetically close to the known m^{3}U RNA methyltransferases. These latter enzymes are exemplified by RlmE, which is responsible for m^{3}U1498 modification in 16S rRNA (Basturea et al. 2006) and belongs to the Cluster of Orthologous Genes family COG1385 within the SPOUT superfamily of AdoMet-dependent methyltransferases (Tkaczuk et al. 2007). Sequence analyses of SPOUT proteins identified two major lineages: one groups several families of known 2′-O-methyltransferases together with the RlmE-type m^{3}U methyltransferases; the second lineage contains TrmD-type and Trm10p-type m^{1}G methyltransferases and the bacterial cluster COG1576, in which YbeA is the sole *E. coli* member (Tkaczuk et al. 2007).

Considering that no m^{1}G RNA methyltransferases remained to be discovered in *E. coli* and that the uridine/pseudouridine

N3-atom can be regarded as being in a structural context that is chemically similar to the guanosine N1-atom (Fig. 1), we deemed YbeA and its COG1576 homologs to be worthy candidates for the task of $m^3\Psi$ methylation. The *ybeA*-knockout was obtained from the Keio collection (Baba et al. 2006). In strain K-12 BW25113 Δ*ybeA*, the putative methyltransferase gene has been replaced with a kanamycin resistance cassette. We confirmed by PCR analysis of the relevant chromosome region that the *ybeA* gene sequence had been displaced.

Detection of a minor growth defect in *ybeA*-knockout cells

The growth rate of the *ybeA*-knockout was measured in rich medium at 37°C to determine whether it differed from that of wild-type or *xylA*-knockout cells. Triplicate measurements in independent cultures under the same conditions showed that the doubling time of the wild-type cells is 34 ± 2 min, *xylA*-knockout cells double in 35 ± 1 min, and *ybeA*-knockout cells take 37 ± 2 min. From these simple growth experiments, we could not with any certainty say whether the doubling times were significantly different.

Growing cells in competition with each other for 50–100 generations in the same culture normally reveals small differences in their doubling times. The wild-type cells were clearly fitter and began to outgrow the *ybeA*-knockout already after the first growth cycle of 10 generations (Fig. 2). To test whether the reduced fitness of *ybeA* cells might merely be due to the cost of expressing the kanamycin resistance gene, growth competition was repeated against *xylA*-knockout cells. The *xylA* cells have the same resistance cassette as the *ybeA*-knockout, and the lack of ability to metabolize xylose should be of no consequence for ribosome biogenesis or for growth in rich medium. The *ybeA* cells were also clearly less fit than *xylA* cells (Fig. 2), although they were not out competed as rapidly as by the wild-type cells.

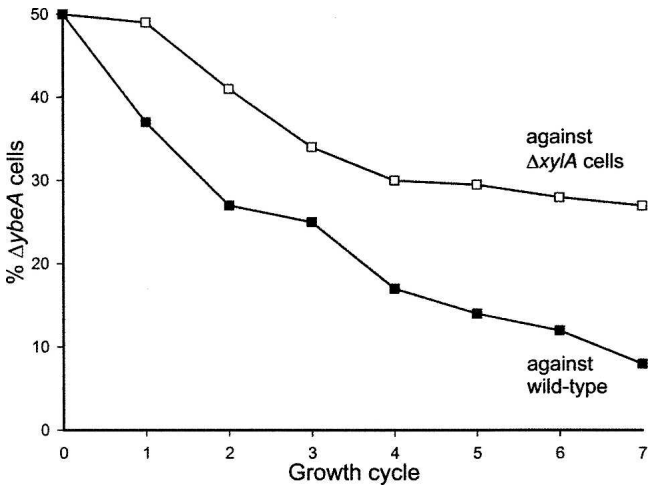

FIGURE 2. Growth of the *ybeA*-knockout (Δ*ybeA*) in competition against wild-type cells or against *xylA*-knockout cells (Δ*xylA*). Equal numbers of viable cells were present at the start of the first growth cycle; each growth cycle represents approximately 10 cell divisions. The values for the relative proportions of cells are averages of duplicate measurements.

Making a straightforward extrapolation from the curves in Figure 2 (i.e., taking no account of potential differences in lag phase times or viability), the growth rate of the *ybeA*-knockout is 5.4% slower than wild-type cells and 2.5% slower than *xylA* cells. If the doubling time of the wild type is set to 34.0 min, the doubling times of the *xylA*- and *ybeA*-knockouts would be 34.7 and 35.5 min, respectively. Thus, the presence of the kanamycin resistance gene does indeed have a biological cost, while loss of *ybeA* function makes its own individual contribution toward slowing growth.

Identification of the YbeA methylation site

The N3-position of uridine and pseudouridine (Fig. 1) is a hydrogen bond donor in canonical Watson–Crick base-pairing interactions, and thus substitution of the N3-proton with a methyl group eliminates its availability for base pairing. The loss of base-pairing ability can be exploited for rapid detection of $m^3\Psi$ (and m^3U) using primer extension analysis, where the progress of reverse transcriptase is impeded by these modifications. We also considered the proviso that the sequence in question at the apex of helix 69 contains three ΨA dinucleotides, and these are linked by notoriously labile phosphodiester bonds. As reverse transcriptase is stopped equally well by backbone cleavage as by $m^3\Psi$ methylation, we initially opted for an analytical method that could unequivocally establish the presence or absence of a methyl group.

MALDI mass spectrometry was applied to determine any difference between methylation patterns in the rRNAs from the wild type and the *ybeA*-knockout. The MALDI-MS approach used here functions optimally on RNA fragments with lengths in the tri- to decanucleotide range, where masses can be accurately measured to within 0.2 Da (Andersen et al. 2004). Thus, molecules as large as the 16S and 23S rRNAs need to be fragmented to yield specific oligonucleotides of suitable size for analysis. In the present study, a 58-nucleotide (nt) sequence from G1891 to G1948 in 23S rRNA was isolated by hybridization to a complementary oligodeoxynucleotide (Fig. 3), and was then fragmented further by RNase digestion. After RNase A digestion, Ψ1915 ends up in an dinucleotide fragment (AΨ) whereas, following RNase T1 digestion, Ψ1915 is in an 11-nt fragment Ψ1911–G1921 that has a unique *m/z* of 3519.5 (unmethylated) or *m/z* of 3533.5 (methylated). In principle, these large oligonucleotides can be identified directly following RNase T1 digestion of total rRNA without prior purification (Madsen et al. 2003). However, isolation of a discrete rRNA region (with the 58-mer) markedly improves the signal-to-noise ratio and gives unambiguous spectra.

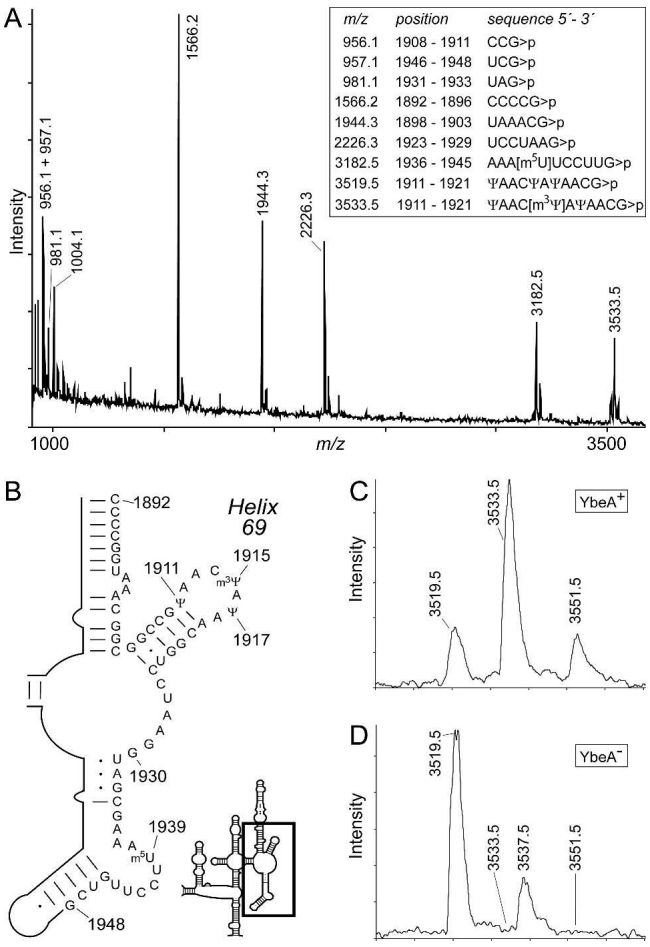

FIGURE 3. MALDI-MS analyses of *E. coli* 23S rRNA around helix 69. The 23S rRNA fragment from nucleotides 1891 to 1948 was isolated from *E. coli* YbeA$^+$ and YbeA$^-$ strains and was then digested with RNase T1. (*A*) MS spectrum of RNA from the YbeA$^+$ strain. The empirically measured masses for RNase T1 digestion products of trinucleotides and larger are shown *above* the peaks and match well with the theoretical values (the theoretical monoisotopic masses are given in the box). In this spectrum, RNase T1 digestion gave rise mainly to products with cyclic phosphates (>p) and a minor amount of linear phosphate products; the linear products, with 18 Da greater masses, can seen immediately to the *right* of the main peaks. Adducts are occasionally evident: e.g., the *m/z* 1004.1 peak is UAG>p with a sodium ion (+23 Da). (*B*) Hairpin 69 region showing the sequence from C1892 to G1948 isolated for MS analysis. The location of the hairpin 69 region is boxed in the outline of the 23S rRNA domain IV secondary structure (Noller 2005). (*C*) Enlargement of the spectral region above *m/z* 3500 from the YbeA$^+$ rRNA. The 11-nt fragment containing $m^3\Psi$1915 runs at *m/z* 3533.5, with a minor linear phosphate component at *m/z* 3551.5. These peaks are preceded by a small, but reproducible, top at *m/z* 3519.5, which is the unmethylated fragment (the linear phosphate component is at *m/z* 3537.5 and hidden in the ^{13}C isotope tail of the more abundant *m/z* 3533.5 peak). The *m/z* 3519.5 peak indicates that the in vivo methylation by YbeA was incomplete. (*D*) The same spectral region from the YbeA$^-$ strain shows that the RNA is entirely in the unmethylated form at *m/z* 3519.5 (with the minor linear phosphate component visible at *m/z* 3537.5). None of the spectral data have been smoothed.

RNase T1 digestion of the isolated 23S rRNA fragment from the wild-type strain produced the *m/z* 3533.5 peak, which has a cyclic phosphate, and a small amount of the linear fragment at *m/z* 3551.5 (Fig. 3C). Both these peaks are consistent with the Ψ1911 to G1921 sequence containing one methyl group. However, a minor quantity of this 11-mer oligonucleotide flew at *m/z* 3519.5, indicating that methylation in wild-type cells was less than stoichiometric. In the *ybeA*-knockout strain, the 11-mer oligonucleotide flew exclusively at *m/z* 3519.5 (with a small amount of the linear fragment at *m/z* 3537.5), showing that in the absence of YbeA there was no methylation in this RNA sequence (Fig. 3D). The *m/z* 3533.5 peak was subjected to further analysis by tandem MS (data not shown), and the site of YbeA methylation was localized to nucleotide 1915.

Stoichiometry of methylation at Ψ 1915 by YbeA

The MALDI-MS analyses on the wild-type and *ybeA*-knockout rRNAs were confirmed by reverse transcriptase primer extension followed by gel analysis, which gives a clear visual illustration of the methylation site (Fig. 4). There is a small amount of reverse transcriptase read-through past $m^3\Psi$1915 (which is stopped at the next modification site, m^2G1835), and this is consistent with the minor proportion of unmethylated rRNA seen with MS for the wild-type rRNA (Fig. 3C). The loss of methylation in the *ybeA*-knockout strain was shown to be rescued by addition of a functional, recombinant version of *ybeA* on a plasmid (Fig. 4). It could be rationalized that Ψ and $m^3\Psi$ could rotate around the glycosidic bond (Fig. 1) and present a *syn* conformation that might facilitate reverse transcriptase read-through. Even so, there are two reasons why we do not believe this happens to any appreciable degree: First, the proportion of unmethylated Ψ1915 in YbeA$^+$ cells estimated by MS and primer extension matches fairly well; second, semi-empirical ab initio calculations using AM1, PM3, and MNDO Hamiltonians suggest that $m^3\Psi$ is unlikely to attain a conformation capable of productive base pairing. In the latter case, no account could be taken for possible water–backbone bridges in the RNA (Sumita et al. 2005) or for interactions within the reverse transcriptase active site. However, for lack of contradictory evidence, we presently equate the amount of reverse transcriptase read-through with the proportion of unmethylated Ψ1915.

Significant read-through past Ψ1915 was observed in the complemented strain (Fig. 4) even though it contained much larger quantities of YbeA enzyme than wild-type cells. We have previously observed for other 23S rRNA methyltransferases, which also fail to completely methylate all the rRNA molecules under normal growth conditions, that stoichiometric rRNA methylation can be achieved if the methyltransferase is expressed in larger quantities. In the case of YbeA, the proportion of 23S rRNA without

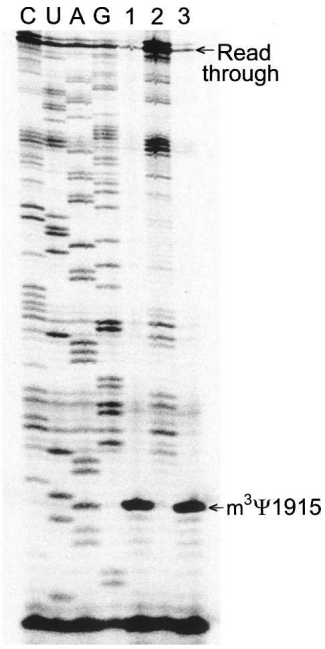

FIGURE 4. Gel autoradiograms of primer extension showing the hairpin 69 region of the rRNAs. (Lane *1*) rRNA was isolated from wild-type *E. coli* (YbeA$^+$, as in Fig. 3C); (lane *2*) rRNA from the *ybeA*-knockout (YbeA$^-$, as in Fig. 3D); (lane *3*) rRNA from the *ybeA*-knockout strain complemented with the plasmid-encoded *ybeA* gene. The transcription stop caused by the N3-methylation at Ψ1915 and the read-through bands are arrowed. Our reasoning (see text) is that reverse transcriptase cannot transcribe past m^{3}Ψ, and thus the read-through band is indicative of unmethylated RNA. The rRNA template for the dideoxy-sequencing reactions (lanes *C*,*U*,*A*,*G*) was from the *ybeA*-knockout.

m^{3}Ψ1915 methylation is seen under logarithmic growth and remains constant even when the intracellular concentration of YbeA is increased (Fig. 4). The explanation that fits best with this observation and the enzyme–target docking (described below) is that the unmethylated faction reflects recently synthesized 23S rRNA molecules that have not yet reached a later stage of assembly where they are recognized by YbeA as suitable substrates.

Sequence analysis of YbeA orthologs

Numerous common motifs are evident in the SPOUT superfamily; some of these motifs are involved in the binding of AdoMet, while others are unique to COG1576 and are probably related to the specific function of YbeA (Fig. 5). YbeA orthologs are present in most major bacterial lineages, and the phylogenetic tree derived from the alignment matches well with the phylogeny of the host organisms (Tkaczuk et al. 2007). In addition to Bacteria, orthologs of *ybeA* are evident in the chloroplasts of numerous plant species; however, these organelles are regarded as being of bacterial origin, and there is no evidence of m^{3}Ψ methylation within the cytoplasmic protein synthesis machinery of Eukaryota. This modification is also essentially absent in the Archaea; however, solitary *ybeA* orthologs have been found within the *Euryarchaeota*, and the significance of this observation remains unclear. On balance, we effectively regard YbeA as being a bacterial enzyme.

None of the organisms mentioned above possesses more than a single COG1576 member, and there is no evidence of species-specific duplication or horizontal gene transfer. Taken together, this would suggest that all YbeA orthologs have the same function. The current extent of the databases shows that every genome that contains a *ybeA* ortholog also contains an ortholog of *rluD*. However, the converse is not true, and *rluD* is found in the genomes of Actinobacteria, Cyanobacteria, and Spirochaetes despite their lack of *ybeA*. This indicates that Ψ formation at nucleotide 1915 is independent of YbeA methylation, whereas the action YbeA might require the prior formation of a Ψ substrate. As the preferred substrate for RluD is the assembled 50S subunit (Leppik et al. 2007; Vaidyanathan et al. 2007), YbeA would methylate Ψ1915 at the same or a later stage of ribosome maturation. Consistent with this, the accompanying article (Ero et al. 2008) shows that YbeA activity requires prior conversion of nucleotide 1915 to pseudouridine and for Ψ1915 to be presented within the context of the 70S ribosome.

A mechanistic model for YbeA activity

To date, four crystal structures of COG1576 members have been determined and deposited in the Protein Data Bank: YbeA from *E. coli* (PDB file 1ns5) (J. Benach, J. Shen, B. Rost, R. Xiao, T. Acton, G. Montelione, and J.F. Hunt, unpubl.), YydA from *Bacillus subtilis* (PDB 1t0o) (A.P. Kuzin, W. Edstrom, S.M. Vorobiev, R. Shastry, L.-C. Ma, R. Xiao, T. Acton, G. T. Montelione, L. Tong, and J.F. Hunt, unpubl.), TM0844 from *Thermotoga maritima* (PDB 1o6d) (Badger et al. 2005), and SAV0024/SA0023 from *Staphylococcus aureus* (PDB 1vh0) (Badger et al. 2005). The proteins display an unusual knotted structure. All SPOUT proteins studied so far crystallize as homodimers, and this is probably the oligomeric state of YbeA in solution (Mallam and Jackson 2007). Details about these proteins are otherwise sparse.

As mentioned above, YbeA and its orthologs are closest relatives of m^{1}G methyltransferases from the TrmD (COG0336) family, and comparisons between crystal structures give DALI Z-scores >11 (Tkaczuk et al. 2007). Thus, findings from structural, biochemical, and mutagenesis studies on TrmD-AdoMet (Ahn et al. 2003; Elkins et al. 2003) can, with caution, be extrapolated to YbeA. Superimposition of YbeA onto the TrmD-AdoMet homodimer suggests that there are near-identical AdoMet-binding pockets in these two proteins. Conserved YbeA residues and a surface of negative charge are evident at the putative AdoMet site, and this site is located adjacent to a surface of positive charge that could interact with the backbone of the

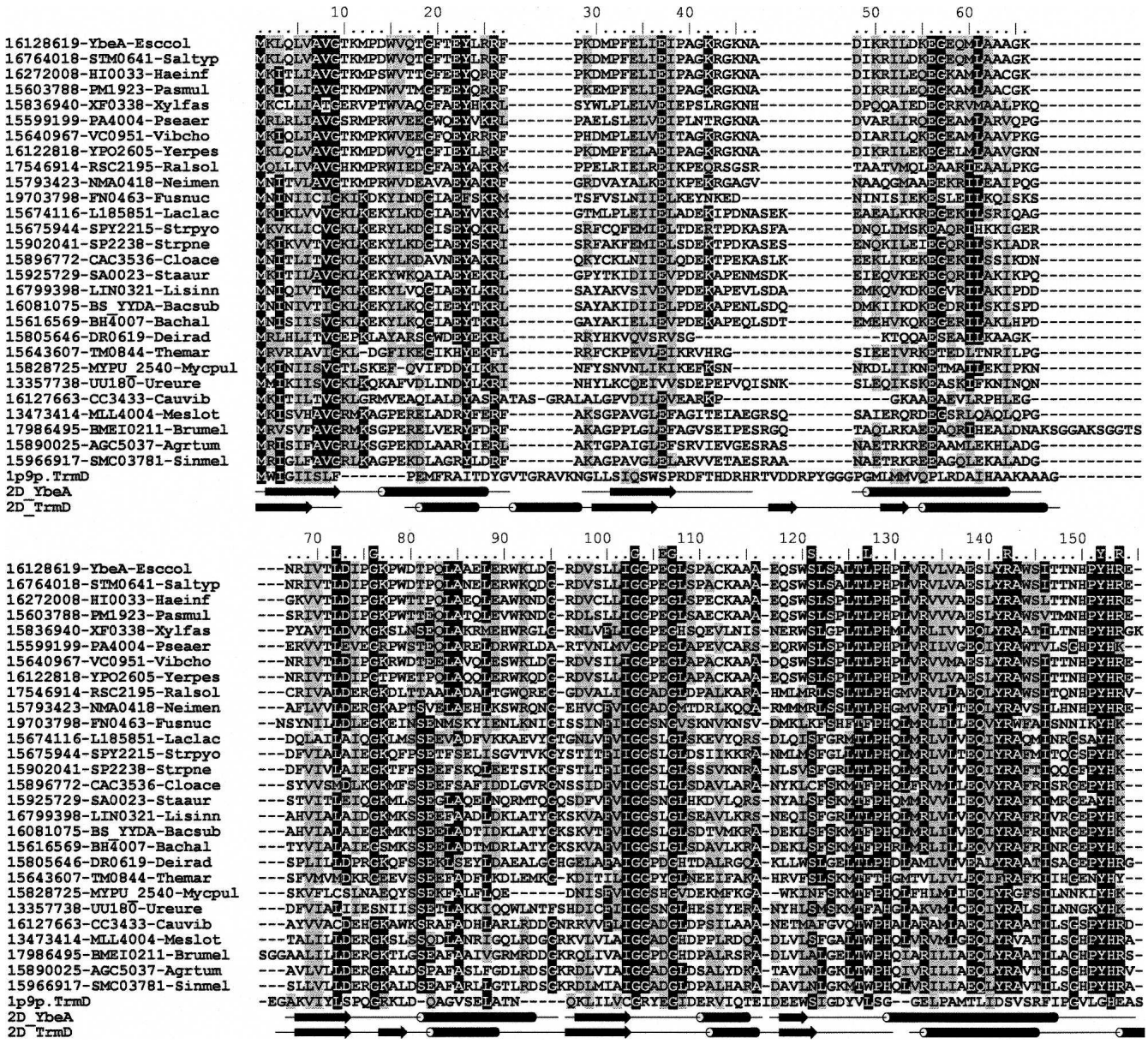

FIGURE 5. Sequence alignment of *E. coli* YbeA with its orthologs from COG1576 and with *E. coli* TrmD, the closest paralog with known function. Conserved and conservatively substituted residues are shaded. Residues L72 to R154 that are putatively directly involved the methylation reactions are indicated *above* the alignment; the extent of α-helical (tubes) and β-sheet secondary structures (arrows) are shown *below* the alignment.

RNA substrate (Fig. 6). The C-terminal domain of TrmD, which probably binds the tRNA substrate, is absent from YbeA; in fact, YbeA lacks any structural elaboration and thus appears to be a minimalist member of the SPOUT superfamily.

A model for the interaction between YbeA-AdoMet and Ψ1915 was generated using the HADDOCK docking program (Dominguez et al. 2003). The proximity between the N3 atom of pseudouridine and the methyl group of AdoMet was used as a spatial constraint and, predictably, places Ψ1915 into the putative active site of YbeA (Fig. 7). The conserved residues L72, G76, G103, G107, S121, and L127 in YbeA respectively correspond to L87, G91, G113, G117, S132, and L138 in TrmD (Fig. 5). YbeA also possesses a number of conserved residues that are spatially equivalent to important TrmD residues, even though they do not coincide in the primary structure alignments. These include YbeA-R142, which seems comparable to TrmD-R154 and might bind the target base, YbeA-R154, which like TrmD-R24 could be involved in RNA backbone interaction, and YbeA-Y152, which might be analogous to TrmD-L160 and possibly stacks upon and stabilizes the target base (Fig. 7). The specificity of YbeA for a pseudouridine substrate (Ero et al. 2008) suggests that base stacking (Davis 1995) and hydrogen bonding with the N1-position

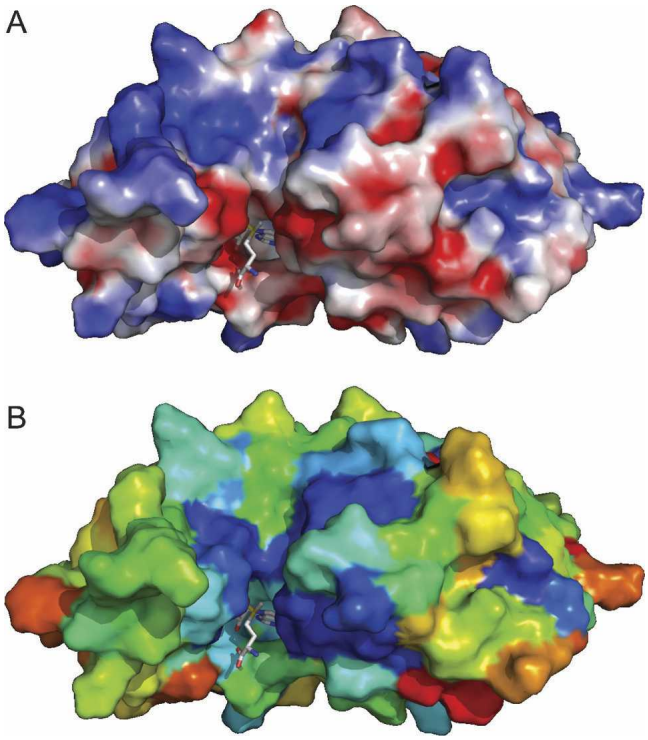

FIGURE 6. Surface representations of a model for the YbeA-AdoMet complex. (*A*) Model colored according to the distribution of electrostatic potential from red (−10 kT) to blue (+10 kT). (*B*) Model colored to show sequence conservation in the COG1576 family: deep blue (invariant) through light blue (conserved), green (similar) to yellow and then red (highly variable). A stick representation of AdoMet is shown (nitrogen atoms, blue; oxygen, red; sulphur, yellow).

are probably important determinants for recognition and methylation of the Ψ1915 target.

There are also obvious differences that could reflect RNA substrate specificities. YbeA-E106 is homologous to TrmD-E116, which is important for target base binding, although E106 is not conserved in the COG1576 family and its side chain is turned away from the active site in YbeA. Surprisingly, there is no obvious YbeA equivalent to TrmD-D169, which was proposed to act as a general base catalyst and deprotonate the N1 atom of guanosine. Possibly a conformational rearrangement is required in YbeA to position another suitable negatively charged residue into the vicinity of the active site.

Interaction of YbeA with the ribosome

Binding of the YbeA dimer to the 70S ribosome (Schuwirth et al. 2005) was investigated computationally using GRAMM (Vakser 1997), which allows rigid body docking with simple criteria for steric and electrostatic compatibility between different kinds of biological macromolecules. A representative structure is shown in Figure 8 from the largest cluster of high-scoring docking solutions that place YbeA active site in the vicinity of the U1915 nucleoside. No attempt has been made to optimize the rigid-body model, and, in the absence of methods to calculate reliable binding energies or conformational changes in protein–RNA complexes, the model should be regarded as preliminary.

Despite this approximation, several striking features are immediately apparent. First, the YbeA dimer makes contacts with both ribosomal subunits. The 30S interactions are extensive and contribute considerably to the orientation and stability of the YbeA interaction; these include contacts to 16S rRNA nucleotides within and adjacent to the decoding site as well as r-protein S12 (Fig. 8, see the legend for details). The 50S subunit contacts are confined to domain IV of 23S rRNA and are mainly in the loop of hairpin 69; YbeA does not come close to any of the 50S subunit proteins. We repeated the docking on the *Thermus thermophilus* 70S ribosome structure (Korostelev et al. 2006), and these simulations placed YbeA in essentially the same position and orientation, although additional 16S rRNA nucleotides (G517–C519 and U531) came within 5 Å of the methyltransferase together with broader stretches of r-protein S12 ($VVRTSL_{51}$, AK_{56}, $HNLQEHS_{80}$) and r-protein S13 residues KK_{121}. The extensive YbeA contacts seen on the 30S subunit match well with the accompanying

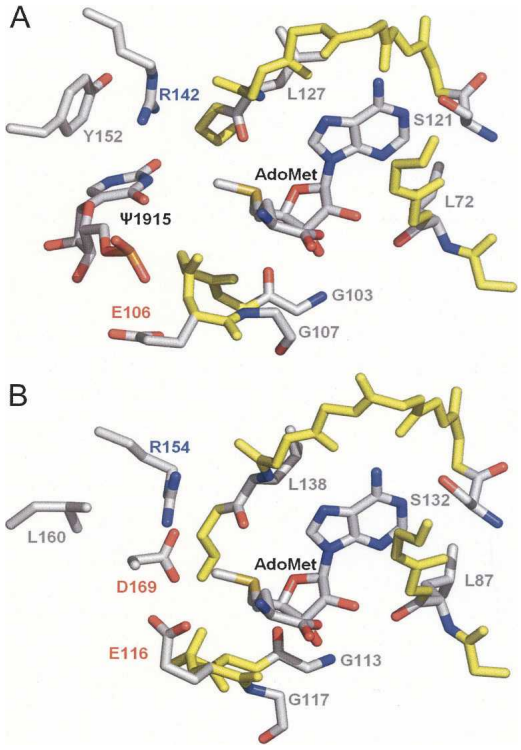

FIGURE 7. (*A*) Docking model of YbeA-AdoMet-Ψ1915 based on (*B*) the TrmD-AdoMet crystal structure. Ligands and side chains of residues potentially involved in the methyl transfer reaction are labeled indicating carbon (gray), nitrogen (blue), and oxygen atoms (red). The backbone of the AdoMet-binding site (conserved between YbeA and TrmD) is indicated in yellow.

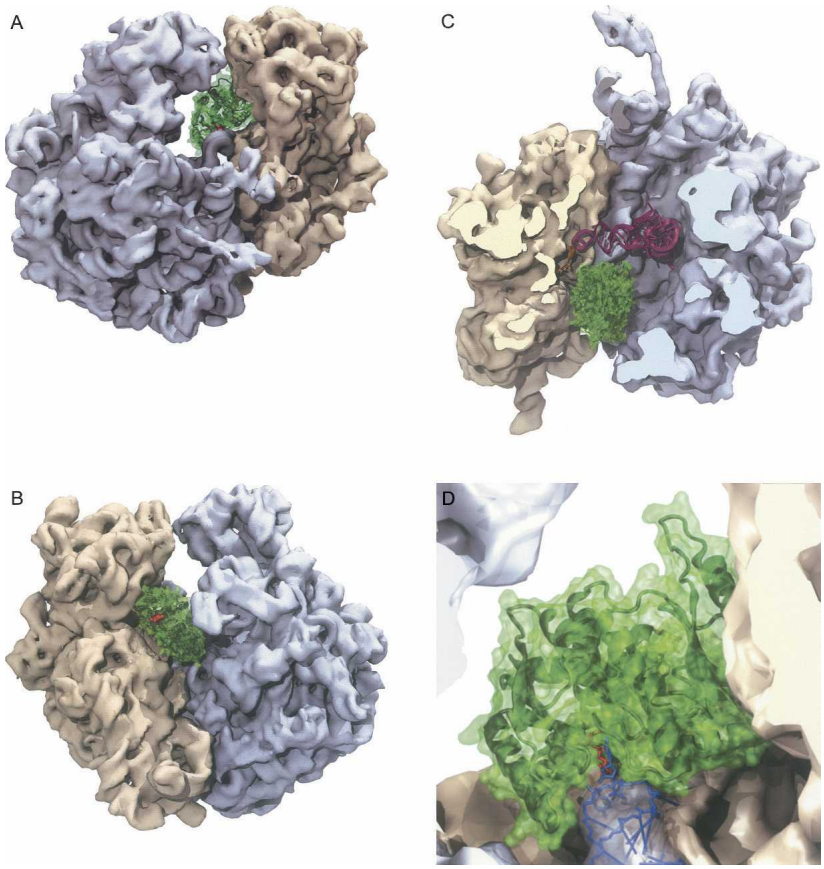

FIGURE 8. Interaction of the YbeA dimer with the *E. coli* 70S ribosome. (*A*) View through the E (exit) site showing how the YbeA methyltransferase (green) fits into the interface between the 50S (gray) and 30S ribosomal subunits (sand). The methylation target Ψ1915 in helix 69 is located adjacent to the AdoMet moiety (red) of YbeA that is visible from this angle. (*B*) View through the A (aminoacyl) site showing the second AdoMet moiety on the YbeA dimer, which appears to be redundant. (*C*) View from above after removal of the 30S head and 50S central protuberance to show the position of YbeA relative the P-site tRNA (magenta) and mRNA (yellow). (*D*) Close up of 23S rRNA helix 69 (blue) showing the methylation target at nucleotide 1915 (light blue stick) and its orientation when flipped (dark blue) into the YbeA active site containing AdoMet (red stick). Residues approaching within 5 Å of YbeA are 16S rRNA nucleotides G953 to G963, C985, U986, U991, C1209 to C1214, A1227, and A1493, 23S rRNA nucleotides A1912–U1917 and U1946, and r-protein S12 residues VYT_{38} and Q_{74}.

study (Ero et al. 2008) showing that YbeA activity requires the 70S ribosome and that the isolated 50S subunit does not function as a suitable methylation substrate.

A second feature of the model is that it offers an explanation for the overall streamlined structure of YbeA and its lack of additional domains. The YbeA structure facilitates the snug fit between the ribosomal subunits where a larger dimer would not be able to access the target. The significance of the dimeric structure is still not fully understood, and we note that the second AdoMet moiety faces out into the solvent at the entry to the A site (Fig. 8B). Another characteristic of the model is that YbeA is positioned where it does not interfere with tRNA binding in the ribosomal P site, but it would occlude tRNA binding in the A site. This might indicate that the physiological substrate is the ribosome initiation complex with fMet-tRNA in the P site. In the top view (Fig. 8C), YbeA can be seen to come close to the anticodon stem of the P-site tRNA and the A-site codon of the mRNA; insufficient data are available at present to assess whether YbeA also contacts these RNAs.

Finally, the model suggests how the methylation reaction might be initiated. The shape complementarity between YbeA and its target site suggests that only a minor change in the rRNA conformation is required to place Ψ1915 into the active site of the enzyme by swinging out the target base into an unstacked configuration (Fig. 8D). Similar base-flipping mechanisms are used by a variety of nucleic acid modification enzymes such as DNA methyltransferases (Klimasauskas et al. 1994), RNA methyltransferases (Lee et al. 2005), and pseudouridine synthases (Hoang and Ferré-D'Amaré 2001).

Assessment of whether such a base-flipping mechanism is used by YbeA will require a crystallographic study of the methyltransferase bound to the 70S ribosome. Other predictions made from this model, including the YbeA–rRNA contacts, could be checked by more readily available techniques such as footprinting. Despite the need for more experimental data, the YbeA substrate requirements taken together with structural considerations lead us to the unavoidable conclusion that the methyltransferase must interact with both ribosomal subunits. YbeA is, to our knowledge, the first example of an rRNA methyltransferase that makes simultaneous contact with both subunits.

In closing, we suggest that a more suitable designation for the SPOUT-superfamily member YbeA would be the **r**RNA **l**arge subunit **m**ethyltransferase RlmH, consistent with the terminology used for the other rRNA methyltransferase characterized in *E. coli* (Ofengand and Del Campo 2004; Andersen and Douthwaite 2006).

MATERIALS AND METHODS

Cloning and knockout of *ybeA*

Cloning of the *ybeA* gene and generation of a knockout strain were carried by Saka et al. (2005) and Baba et al. (2006), respectively; the recombinant plasmid and the knockout strain were obtained

from the Keio collection (Baba et al. 2006). Briefly, the full-length *ybeA* gene was cloned on a plasmid under control of the *lac* promoter, and the recombinant YbeA protein is expressed with a C-terminal histidine tag. The *ybeA* gene in *E. coli* K-12 strain BW25113 was replaced with a kanamycin cassette flanked by FRT sites (Flp recombination target) in a one-step, site-specific recombination event creating an in-frame deletion of the entire *ybeA* gene.

The structure of the relevant chromosomal region of the BW25113 Δ*ybeA* strain was confirmed by PCR sequencing, and the structure of plasmid pCA24N *ybeA*$^+$ was verified by a combination of restriction enzyme mapping and sequencing. Restriction endonucleases and other enzymes for DNA manipulations (Fermentas) were used according to the suppliers' recommendations; plasmid DNA was isolated by using a plasmid miniprep kit (Qiagen); *E. coli* transformations were performed by standard methods (Sambrook et al. 1989).

Growth experiments

The growth rates of the wild-type and *ybeA*-knockout strains were determined during exponential growth phase in triplicate cultures at 37°C in rich (LB) liquid medium.(Sambrook et al. 1989). Overnight cultures were diluted to an optical density (A_{450}) of 0.01, and growth was monitored spectroscopically every 20 min.

Growth competition experiments were performed in duplicate as previously described (Gutgsell et al. 2000; Toh et al. 2008) starting with approximately equal numbers of *xylA*- and *ybeA*-knockout cells at the same growth phase or, alternatively, starting under the same conditions with wild-type and *ybeA*-knockout cells. The *xylA* gene in the growth comparator had been inactivated with the same kanamycin resistance cassette used in the *ybeA* strain, and, in theory, *xylA* cells should grow at the same rate as the wild-type strain in rich medium unless expression of the resistance cassette has a biological cost. Growth competition was followed in rich (LB) liquid medium (Sambrook et al. 1989) at 37°C. At the end of every 6-h cycle, cells were diluted to an A_{450} of 0.01 in fresh medium. The relative numbers of *ybeA* and *xylA* cells were followed throughout the growth cycles by plating on MacConkey agar supplemented with 1% (w/v) D-xylose (Toh et al. 2008), and also on MacConkey/xylose agar with kanamycin at 50 mg/L, and screening for red and white colonies. In parallel experiments, the relative numbers of wild-type and *ybeA* cells were estimated by plating on LB agar (where all cells grow) and LB agar with kanamycin at 50 mg/L (only the *ybeA* cells grow).

Analysis of rRNA by MALDI mass spectrometry

Total rRNA was extracted from ribosomal particles isolated from *E. coli* wild-type and *ybeA*-knockout strains. The defined rRNA sequence from G1891 to G1948 in 23S rRNA was isolated by hybridization to a complementary 58-mer deoxyoligonucleotide (Andersen et al. 2004; Douthwaite and Kirpekar 2007). Briefly, 100 pmol of total rRNA were heated with 400 pmol of deoxyoligonucleotide at 85°C for 1 min, followed by slow cooling to 45°C over 2 h. Regions of the rRNAs that were not protected by hybridization were digested away with Mung bean nuclease (NE Biolabs) and RNase A (Sigma), and the rRNA sequence paired to the deoxyoligonucleotide was separated by gel electrophoresis and then extracted. The rRNA sequence of ~58 nt was digested with 20 units of RNase T1 (USB) at 37°C for 3 h in 2 μL H_2O containing 0.25 μL of 0.5 M 3-hydroxypicolinic acid. Samples were dried and resuspended in 1 μL H_2O prior to analysis by MALDI-MS (Voyager Elite, Perseptive Biosystems) recording in reflector and positive ion mode (Kirpekar et al. 2000). Spectra were analyzed using the program m/z (Proteometrics Inc). Tandem mass spectra were recorded in positive ion mode on a MicroMass MALDI Q-TOF Ultima mass spectrometer as previously described (Kirpekar and Krogh 2001).

Primer extension

A deoxynucleotide primer complementary to the 1925 to 1942 region of *E. coli* 23S rRNA was 5′-end-labeled with ^{32}P (and in later experiments with ^{33}P), hybridized to rRNA samples and extended with AMV reverse transcriptase (Finnzymes) as described by Stern et al. (1988). Extension products were run on polyacrylamide/urea gels alongside dideoxy sequencing reactions performed on rRNA from the *ybeA*-knockout strain to ensure read-through past U1915. Gels bands were visualized by phosphorimaging (Typhoon, Amersham Biosciences).

Molecular modeling and docking

The YbeA protein structure was analyzed and visualized with the PyMol molecular graphics system (http://www.pymol.org) and VMD (Humphrey et al. 1996); calculations of the electrostatic potential were carried out with APBS tools. Sequence conservation was mapped onto the model via the COLORADO3D server (Sasin and Bujnicki 2004), using the Rate4Site method, with the JTT substitution matrix and ML model for rate inference. The model of protein–pseudouridine complex was constructed with the docking method HADDOCK (Dominguez et al. 2003).

GRAMM v1.03 (Vakser 1997) was used for rigid-body docking of the *E. coli* YbeA dimer (crystal structure 1ns5) to the *E. coli* 70S ribosome (Schuwirth et al. 2005). The PDB files used for the ribosome structure were as follows: 30S subunit, 2AVY and 2I2P; 50S subunit 2AW4 and 2I2T. The truncated anticodon stem–loop structure was aligned with the P-site tRNA from the *T. thermophilus* 70S ribosome structure, 1GIX (Yusupov et al. 2001). All docking simulations were repeated with the *T. thermophilus* 70S ribosome structure (Korostelev et al. 2006), with essentially the same result. In all simulations, the high-resolution docking mode was used to generate 1000 alternative orientations that optimized the steric and electrostatic complementarity between the ribosome and YbeA structures. These alternative models were subsequently ranked according to the proximity between the putative active site of YbeA (as inferred from earlier docking analyses of AdoMet and Ψ1915) and the position of U1915 in the ribosome structure. The ranking was carried out with the FILTREST3D method (M.J. Gajda and J.M. Bujnicki, in prep.; a web server is available at http://filtrest3d.genesilico.pl/filtrest3d/index.html). One hundred top-scoring models (those with the active site of YbeA close to U1915 in the ribosome) were clustered using the MAXCLUSTER method (http://www.sbg.bio.ic.ac.uk/~maxcluster/index.html), and the central conformation from largest cluster was selected as the most preferred orientation.

SUPPLEMENTAL DATA

Data from the ribosome docking simulations are available as supplementary material at http://www.rnajournal.org.

ACKNOWLEDGMENTS

We thank Anette Rasmussen, Michelle O'Connor, Jacob Poehlsgaard, and Finn Kirpekar for help and advice with data interpretation. We are indebted to Jaanus Remme for revealing to us that 70S and not 50S is the substrate for YbeA methylation (see accompanying article Ero et al. 2008). S.D. gratefully acknowledges support from the Danish Research Agency (FNU-rammebevilling 272-07-0613), the Nucleic Acid Center of the Danish Grundforskningsfond, and NAC-DRUG under the FP6 Marie Curie Initial Training Networks (to E.P). Support was provided to J.M.B., K.H.K., J.M.K. and E.P. by the Polish Ministry of Science (grant N301 2396 33).

Received May 30, 2008; accepted July 9, 2008.

REFERENCES

Ahn, H.J., Kim, H.W., Yoon, H.J., Lee, B.I., Suh, S.W., and Yang, J.K. 2003. Crystal structure of tRNA(m^1G37)methyltransferase: Insights into tRNA recognition. *EMBO J.* **22:** 2593–2603.

Ali, I.K., Lancaster, L., Feinberg, J., Joseph, S., and Noller, H.F. 2006. Deletion of a conserved, central ribosomal intersubunit RNA bridge. *Mol. Cell* **23:** 865–874.

Andersen, N.M. and Douthwaite, S. 2006. YebU is a m^5C methyltransferase specific for 16S rRNA nucleotide 1407. *J. Mol. Biol.* **359:** 777–786.

Andersen, T.E., Porse, B.T., and Kirpekar, F. 2004. A novel partial modification at C2501 in *Escherichia coli* 23S ribosomal RNA. *RNA* **10:** 907–913.

Baba, T., Ara, T., Hasegawa, M., Takai, Y., Okumura, Y., Baba, M., Datsenko, K.A., Tomita, M., Wanner, B.L., and Mori, H. 2006. Construction of *Escherichia coli* K-12 in-frame, single-gene knockout mutants: The Keio collection. *Mol. Syst. Biol.* **2:** doi: 10.1038/msb4100050.

Badger, J., Sauder, J.M., Adams, J.M., Antonysamy, S., Bain, K., Bergseid, M.G., Buchanan, S.G., Buchanan, M.D., Batiyenko, Y., Christopher, J.A., et al. 2005. Structural analysis of a set of proteins resulting from a bacterial genomics project. *Proteins* **60:** 787–796.

Ban, N., Nissen, P., Hansen, J., Moore, P.B., and Steitz, T.A. 2000. The complete atomic structure of the large ribosomal subunit at 2.4 Å resolution. *Science* **289:** 905–920.

Basturea, G.N., Rudd, K.E., and Deutscher, M.P. 2006. Identification and characterization of RsmE, the founding member of a new RNA base methyltransferase family. *RNA* **12:** 426–434.

Brimacombe, R., Mitchell, P., Osswald, M., Stade, K., and Bochkariov, D. 1993. Clustering of modified nucleotides at the functional center of bacterial ribosomal RNA. *FASEB J.* **7:** 161–167.

Davis, D.R. 1995. Stabilization of RNA stacking by pseudouridine. *Nucleic Acids Res.* **23:** 5020–5026.

Decatur, W.A. and Fournier, M.J. 2002. rRNA modifications and ribosome function. *Trends Biochem. Sci.* **27:** 344–351.

Dominguez, C., Boelens, R., and Bonvin, A.M. 2003. HADDOCK: A protein–protein docking approach based on biochemical or biophysical information. *J. Am. Chem. Soc.* **125:** 1731–1737.

Douthwaite, S. and Kirpekar, F. 2007. Identifying modifications in RNA by MALDI mass spectrometry. *Methods Enzymol.* **425:** 1–20.

Ejby, M., Sorensen, M.A., and Pedersen, S. 2007. Pseudouridylation of helix 69 of 23S rRNA is necessary for an effective translation termination. *Proc. Natl. Acad. Sci.* **104:** 19410–19415.

Elkins, P.A., Watts, J.M., Zalacain, M., van Thiel, A., Vitazka, P.R., Redlak, M., Andraos-Selim, C., Rastinejad, F., and Holmes, W.M. 2003. Insights into catalysis by a knotted TrmD tRNA methyltransferase. *J. Mol. Biol.* **333:** 931–949. doi: 10.1261/rna.1186608.

Ero, R., Peil, L., Liiv, A., and Remme, J. 2008. Identification of pseudouridine methyltransferase in *Escherichia coli*. *RNA* (this issue). doi: 10.1261/rna.1186608.

Grosjean, H. 2005. *Fine-tuning of RNA functions by modification and editing. Topics in current genetics* (ed. S. Hohmann), Vol. 12. Springer, New York.

Gutgsell, N., Englund, N., Niu, L., Kaya, Y., Lane, B.G., and Ofengand, J. 2000. Deletion of the *Escherichia coli* pseudouridine synthase gene *truB* blocks formation of pseudouridine 55 in tRNA in vivo, does not affect exponential growth, but confers a strong selective disadvantage in competition with wild-type cells. *RNA* **6:** 1870–1881.

Gutgsell, N.S., Del Campo, M., Raychaudhuri, S., and Ofengand, J. 2001. A second function for pseudouridine synthases: A point mutant of RluD unable to form pseudouridines 1911, 1915, and 1917 in *Escherichia coli* 23S ribosomal RNA restores normal growth to an RluD-minus strain. *RNA* **7:** 990–998.

Harms, J., Schluenzen, F., Zarivach, R., Bashan, A., Gat, S., Agmon, I., Bartels, H., Franceschi, F., and Yonath, A. 2001. High resolution structure of the large ribosomal subunit from a mesophilic eubacterium. *Cell* **107:** 679–688.

Hirabayashi, N., Sato, N.S., and Suzuki, T. 2006. Conserved loop sequence of helix 69 in *Escherichia coli* 23S rRNA is involved in A-site tRNA binding and translational fidelity. *J. Biol. Chem.* **281:** 17203–17211.

Hoang, C. and Ferré-D'Amaré, A.R. 2001. Cocrystal structure of a tRNA Psi55 pseudouridine synthase: Nucleotide flipping by an RNA-modifying enzyme. *Cell* **107:** 929–939.

Humphrey, W., Dalke, A., and Schulten, K. 1996. VMD: Visual molecular dynamics. *J. Mol. Graph.* **14:** 33–38.

Johansen, S.K., Maus, C.E., Plikaytis, B.B., and Douthwaite, S. 2006. Capreomycin binds across the ribosomal subunit interface using *tlyA*-encoded 2′-*O*-methylations in 16S and 23S rRNAs. *Mol. Cell* **23:** 173–182.

Kirpekar, F. and Krogh, T.N. 2001. RNA fragmentation studied in a matrix-assisted laser desorption/ionisation tandem quadropole/orthogonal time-of-flight mass spectrometer. *Rapid Commun. Mass Spectrom.* **15:** 8–14.

Kirpekar, F., Douthwaite, S., and Roepstorff, P. 2000. Mapping post-transcriptional modifications in 5S ribosomal RNA by MALDI mass spectrometry. *RNA* **6:** 296–306.

Kiss, T. 2001. Small nucleolar RNA-guided post-transcriptional modification of cellular RNAs. *EMBO J.* **20:** 3617–3622.

Klimasauskas, S., Kumar, S., Roberts, R.J., and Cheng, X. 1994. HhaI methyltransferase flips its target base out of the DNA helix. *Cell* **76:** 357–369.

Korostelev, A., Trakhanov, S., Laurberg, M., and Noller, H.F. 2006. Crystal structure of a 70S ribosome-tRNA complex reveals functional interactions and rearrangements. *Cell* **126:** 1065–1077.

Kowalak, J.A., Bruenger, E., Hashizume, T., Peltier, J.M., Ofengand, J., and McCloskey, J.A. 1996. Structural characterization of U*-1915 in domain IV from *Escherichia coli* 23S ribosomal RNA as 3-methylpseudouridine. *Nucleic Acids Res.* **24:** 688–693.

Lafontaine, D.L. and Tollervey, D. 1998. Birth of the snoRNPs: The evolution of the modification-guide snoRNAs. *Trends Biochem. Sci.* **23:** 383–388.

Lee, T.T., Agarwalla, S., and Stroud, R.M. 2005. A unique RNA fold in the RumA-RNA-cofactor ternary complex contributes to substrate selectivity and enzymatic function. *Cell* **120:** 599–611.

Leppik, M., Peil, L., Kipper, K., Liiv, A., and Remme, J. 2007. Substrate specificity of the pseudouridine synthase RluD in *Escherichia coli*. *FEBS J.* **274:** 5759–5766.

Liiv, A., Karitkina, D., Maivali, U., and Remme, J. 2005. Analysis of the function of *E. coli* 23S rRNA helix-loop 69 by mutagenesis. *BMC Mol. Biol.* **6:** 18.

Madsen, C.T., Mengel-Jorgensen, J., Kirpekar, F., and Douthwaite, S. 2003. Identifying the methyltransferases for m^5U747 and m^5U1939 in 23S rRNA using MALDI mass spectrometry. *Nucleic Acids Res.* **31:** 4738–4746.

Mallam, A.L. and Jackson, S.E. 2007. A comparison of the folding of two knotted proteins: YbeA and YibK. *J. Mol. Biol.* **366:** 650–665.
Noller, H.F. 2005. RNA structure: Reading the ribosome. *Science* **309:** 1508–1514.
O'Connor, M. 2007. Interaction between the ribosomal subunits: 16S rRNA suppressors of the lethal ΔA1916 mutation in the 23S rRNA of *Escherichia coli*. *Mol. Genet. Genomics* **278:** 307–315.
O'Connor, M. and Dahlberg, A.E. 1995. The involvement of two distinct regions of 23S ribosomal RNA in tRNA selection. *J. Mol. Biol.* **254:** 838–847.
Ofengand, J. and Del Campo, M 2004. Modified nucleotides of *Escherichia coli* ribosomal RNA. In *EcoSal*—Escherichia coli *and* Salmonella: *Cellular and molecular biology* (ed. R. Curtiss). ASM Press, Washington, DC.
Rozenski, J., Crain, P.F., and McCloskey, J.A. 1999. The RNA Modification Database: 1999 update. *Nucleic Acids Res.* **27:** 196–197.
Saka, K., Tadenuma, M., Nakade, S., Tanaka, N., Sugawara, H., Nishikawa, K., Ichiyoshi, N., Kitagawa, M., Mori, H., Ogasawara, N., et al. 2005. A complete set of *Escherichia coli* open reading frames in mobile plasmids facilitating genetic studies. *DNA Res.* **12:** 63–68.
Sambrook, J., Fritsch, E.F., and Maniatis, T. 1989. *Molecular cloning: A laboratory manual*. Cold Spring Harbor Laboratory Press, Cold Spring Harbor, New York.
Sasin, J.M. and Bujnicki, J.M. 2004. COLORADO3D, a web server for the visual analysis of protein structures. *Nucleic Acids Res.* **32:** W586–W589.
Schuwirth, B.S., Borovinskaya, M.A., Hau, C.W., Zhang, W., Vila-Sanjurjo, A., Holton, J.M., and Cate, J.H. 2005. Structures of the bacterial ribosome at 3.5 Å resolution. *Science* **310:** 827–834.
Selmer, M., Dunham, C.M., Murphy, F.V., Weixlbaumer, A., Petry, S., Kelley, A.C., Weir, J.R., and Ramakrishnan, V. 2006. Structure of the 70S ribosome complexed with mRNA and tRNA. *Science* **313:** 1935–1942.
Sergiev, P.V., Bogdanov, A.A., and Dontsova, O.A. 2007. Ribosomal RNA guanine-(N2)-methyltransferases and their targets. *Nucleic Acids Res.* **35:** 2295–2301.
Stern, S., Moazed, D., and Noller, H.F. 1988. Structural analysis of RNA using chemical and enzymatic probing monitored by primer extension. *Methods Enzymol.* **164:** 481–489.
Sumita, M., Desaulniers, J.P., Chang, Y.C., Chui, H.M., Clos, L., and Chow, C.S. 2005. Effects of nucleotide substitution and modification on the stability and structure of helix 69 from 28S rRNA. *RNA* **11:** 1420–1429.
Tkaczuk, K.L., Dunin-Horkawicz, S., Purta, E., and Bujnicki, J.M. 2007. Structural and evolutionary bioinformatics of the SPOUT superfamily of methyltransferases. *BMC Bioinformatics* **8:** 73.
Toh, S.-M., Xiong, L., Bae, T., and Mankin, A.S. 2008. The methyltransferase YfgB/RlmN is responsible for modification of adenosine 2503 in 23S rRNA. *RNA* **14:** 98–106.
Tran, E., Brown, J., and Maxwell, E.S. 2004. Evolutionary origins of the RNA-guided nucleotide-modification complexes: From the primitive translation apparatus? *Trends Biochem. Sci.* **29:** 343–350.
Vaidyanathan, P.P., Deutscher, M.P., and Malhotra, A. 2007. RluD, a highly conserved pseudouridine synthase, modifies 50S subunits more specifically and efficiently than free 23S rRNA. *RNA* **13:** 1868–1876.
Vakser, I.A. 1997. Evaluation of GRAMM low-resolution docking methodology on the hemagglutinin-antibody complex. *Proteins* Suppl 1: 226–230.
Yusupov, M.M., Yusupova, G.Z., Baucom, A., Lieberman, K., Earnest, T.N., Cate, J.H., and Noller, H.F. 2001. Crystal structure of the ribosome at 5.5 Å resolution. *Science* **292:** 883–896.